Journal of Chromatography A, 1217 (2010) 7593–7597

Contents lists available at ScienceDirect

Journal of Chromatography A

journal homepage: www.elsevier.com/locate/chroma

Capillary zone electrophoresis of graphene oxide and chemically converted graphene

Marc B. Müller[a,1], Joselito P. Quirino[b,*], Pavel N. Nesterenko[b,*], Paul R. Haddad[b,2], Sanjeev Gambhir[a,1], Dan Li[c], Gordon G. Wallace[a,1]

[a] ARC Centre of Excellence for Electromaterials Science, Intelligent Polymer Research Institute, University of Wollongong, NSW 2522, Australia
[b] Australian Centre for Research on Separation Science, School of Chemistry, University of Tasmania, Private Bag 75, Hobart, Tasmania, Australia
[c] Department of Materials Engineering, ARC Centre of Excellence for Electromaterials Science, Monash University, Clayton, VIC 3800, Australia

ARTICLE INFO

Article history:
Received 27 July 2010
Received in revised form
21 September 2010
Accepted 27 September 2010

Keywords:
Capillary zone electrophoresis
Graphene nanosheets
Fractionation
Aggregation
Atomic force microscopy
Sonication

ABSTRACT

The preparation of processable graphene oxide colloids called chemically converted graphene (CCG) involves the following steps: oxidation of graphite to form graphite oxide; exfoliation of graphite oxide to form graphene oxide (GO); and reduction of GO to form CCG. In this work, the exfoliation and reduction steps were monitored by capillary zone electrophoresis (CZE). CZE was performed in fused silica capillaries with UV absorbance at 230 nm (GO) and 270 nm (CCG) using 250 μM tetrapropylammonium hydroxide (pH 10.4). The results indicate that almost complete exfoliation of graphite oxide (0.05 wt%) and higher recovery of CCG were obtained by sonication at 50% power for more than 15 h. CZE is considered a valuable tool for the fractionation and analysis of GO nanoparticles and, hence, for the control of different steps in preparation of CCG.

1. Introduction

Graphene is a class of two-dimensional nano- to micrometer sized polyaromatic molecules with remarkable thermal, mechanical, and electric properties, which makes it a good candidate for a wide variety of technical applications [1]. Designing graphene materials for applications, using nanoengineering techniques such as self-assembly, depends critically on the attached functional groups and the size of the graphene sheets, which determine the graphene dispersion stability, optical and electrical properties, surface roughness, hardness and tensile strength of the corresponding nanocomposite products. Therefore, the fractionation and analysis of graphene nanosheet distribution based on functionalisation and sheet size is of great importance.

Capillary electrophoresis (CE) is a simple, high efficiency, low sample and solvent consumption separation technique that is applicable to almost any types of analytes. We chose capillary zone electrophoresis (CZE), a separation technique of the CE family, for analysis of aqueous dispersions of colloidal graphene nanosheets. In CZE, the analyte particles and background electrolyte (BGE) move freely through the capillary driven only by the electric field, resulting in separation of the analytes according to charge and flow resistance (i.e. shape, volume and mass). CE separations have been performed on micro- to nano-materials such as metal oxides [2], gold nanoparticles [3], silica [4], latexes [5], carbon nanotubes [6–9], carbon nanoparticles from soot [10], and quantum dots [11]. CZE provides extremely important information about size, charge and shapes of various nanoparticles and, sometimes, it is only possibility to separate them.

However, it should be noted that these separations involve spheres or rods and not flat sheets as encountered with graphene dispersions. The separation mechanism based on electrophoretic mobility that is a function of the zeta potential in the CE analysis of spherical particles may be applied to graphene sheets. The migration of particles in the electric field depends on the particle's surface charge density and the ionic strength of the BGE [12,13]. In addition, the two-dimensional (2D) shape makes graphene very orientation dependent with regard to direction of flow. The irregular shape (e.g. not square or round) and the different functional groups at the surfaces of the basal planes and edges of graphene sheets cause electrophoretic heterogeneity that results in broad peaks should also be considered in the CE analysis [11,14].

* Corresponding authors. Tel.: +61 03 6226 2165; fax: +61 03 6226 2858.
E-mail addresses: jquirino@utas.edu.au (J.P. Quirino), Pavel.Nesterenko@utas.edu.au (P.N. Nesterenko), gwallace@uow.edu.au (G.G. Wallace).
[1] Tel.: +61 02 4221 3127; fax: +61 02 4221 3114.
[2] Tel.: +61 03 6226 2165; fax: +61 03 6226 2858.

0021-9673/$ – see front matter.
doi:10.1016/j.chroma.2010.09.069

We investigated two types of graphene nanosheets, the non-conducting graphene oxide (GO) and the conducting chemically converted graphene (CCG), both in the form of aqueous dispersions. We developed CCG dispersions as a simple approach to the large-scale production of processable aqueous graphene dispersions, without the need for stabilizers [15]. The solution based approach involves the chemical oxidation of graphite to hydrophilic graphite oxide that is exfoliated by ultrasonication in water to form individual graphene oxide (GO) sheets [1,15]. The GO sheets formed contain mostly epoxide and hydroxyl groups in their basal planes and hydroxyl, carbonyl and carboxyl groups at the edges [15–18]. The idealized structure proposed for GO is shown in Supplementary Information Figure 1. After separating graphite by oxidation and exfoliation into graphene oxide, it can be deoxygenated by addition of hydrazine to form CCG. Though the exact reduction process is unknown, the amount of oxygen and oxygen based functional groups is reduced and sp^2 bonds are restored, making CCG electrically conducting while GO is almost entirely insulating [19]. CCG contains less acid groups than GO and therefore shows a less negative zeta potential, but CCG nanoparticles can be more polarized in the electric field resulting in formation of big dipoles.

Here, we report the use of CZE for the analysis of graphene oxide colloids obtained from the exfoliation and reduction steps involved in the preparation of CCG. Four different colloidal GO and CCG dispersions of different size graphene sheets were investigated.

2. Materials and methods

2.1. Chemicals and reagents

The BGE was prepared by diluting or dissolving an appropriate amount of analytical grade tetrapropylammonium hydroxide or ammonium acetate in Milli-Q water. All BGEs were degassed before being used. GO was prepared from purified natural graphite (Bay Carbon, SP-1, with a nominal particle size of 30 μm) using a modified Hummers method [20,21]. CCG was synthesized as we described earlier [15].

2.2. Graphene nanosheets preparation and AFM analysis

Three GO dispersions with different particle size distributions, described as GO1, GO2, GO3 in order of decreasing size, were prepared from oxidized graphite. An untreated graphite oxide was labeled as GO0. In addition, a GOx sample was used to study the effects of ammonium acetate concentration on the CZE profile. Sheet size was controlled through sonication power and centrifugation as shown in Supplementary Information Table 1 (Branson Digital Sonifier 450, Sigma Laboratory Centrifuges 4-15). All GO dispersions were cooled and stayed between 10 °C and 40 °C during sonication. Sonication promotes the exfoliation of stacked graphene oxide sheets in oxidized graphite. Centrifugation allows separation of heavy from light particles, as well as non-colloidal, i.e. non-functionalised from colloidal particles. GOx was centrifuged at 1400 rcf for 30 min to remove non-exfoliated GO particles. One more sample GO3a was produced the same way as GO3 by additional centrifugation for 15 min at 500 rcf to remove pieces of carbon sheets that do not contain sufficient functional groups to keep them dispersed. Some of these non-functionalised particles settled down in the GO3 dispersion but could be redispersed for a short period of time by shaking the sample. This finding supports the theory that graphene oxide contains regimes of non-functionalised polyaromatic graphene structures in its basal plane that can be broken off by sonication and settles down due to hydrophobicity and low polarity [22]. Reduction of GO and CCG with hydrazine was performed as described for GO in Ref. [12].

Sheet size was determined by atomic force microscopy (AFM) using an Asylum MFP 3D and Igor Pro analysis software. The AFM images of GO nanosheets look the same as for the CCG nanosheets as the chemical reduction of GO to CCG does not change the sheet size apart from removing or changing attached functional groups. The AFM images that show the shape and approximate size of GO0, GO1, GO2, and GO3 are shown in Fig. 1. The average sizes of particles are listed in Supplementary Information Table 1.

2.3. Capillary zone electrophoresis

An Agilent CE system Model G1600AX was used to perform the separation together with the included 3D-CE Chemstation software to collect and analyse the data. A photodiode array detector was set

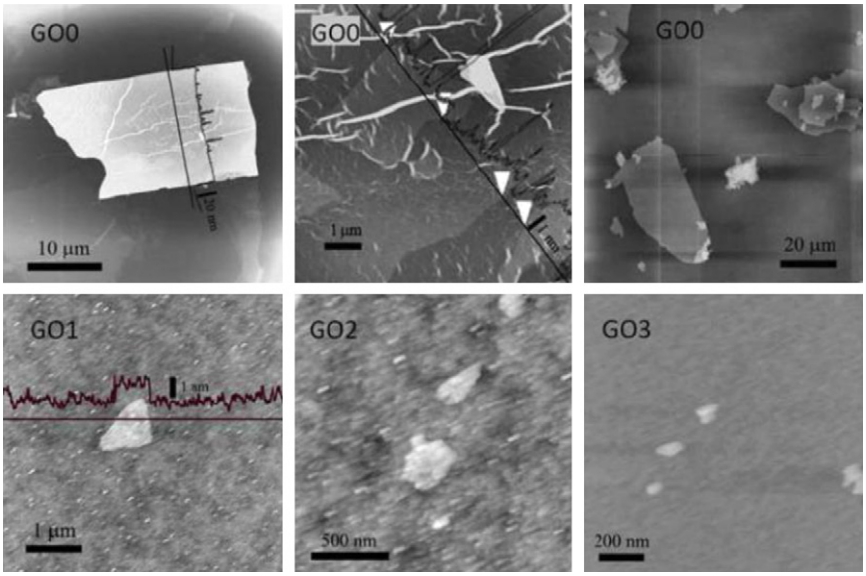

Fig. 1. Atomic force micrographs of graphene oxide samples GO0, GO1, GO2, GO3 on silicon wafer with height cross-sections along the indicated lines. The first row shows the exfoliation of GO without sonication. The top middle image is a magnified view of the non-exfoliated GO particle on the top left, where single graphene oxide sheets start to peel off. The second row shows the effect of longer sonication times creating smaller sheets.

to detect at the maximum absorbance of GO and CCG, at 230 nm and 270 nm respectively. The fused silica capillary was obtained from Polymicro Technologies, Phoenix, AZ. The detection window was created by removing the polyimide coating with hot, concentrated sulphuric acid. The capillary was initialized with 10 min 0.1 M NaOH rinsing, 5 min deionised water, and 5 min BGE prior to each use. In between the runs the capillary was rinsed first for 5 min each with deionised water and BGE. A fresh BGE was used for each electrophoretic run. The capillary temperature was set at 22 °C. The GO and CCG sample dispersions each were 0.05 wt% in deionised water.

Effect of buffer concentration on the electrophoretic profiles was studied using the GOx sample with the following CZE conditions: 20 cm (effective length 11.5 cm) × 50 μm ID × 365 μm OD capillary, injection at 50 mbar for 5 s, and separation voltage at 20 kV. 2 and 5 mM ammonium acetate solutions were prepared from a 10 mM ammonium acetate all having a pH of 7.0.

For succeeding experiments, a 50 cm (effective length 41.5 cm) × 75 μm ID × 365 μm OD capillary, injection at 50 mbar for 5 s, and separation voltage at 15 kV, and a low ionic strength buffer, 250 μM tetrapropylammonium hydroxide (pH 10.4) was used for the CZE analysis of GO0, GO1, GO2, GO3, and GO3a and their reduced counterparts CCG0, CCG1, CCG2, CCG3, CCG3a.

3. Results and discussion

3.1. Selection of BGE for CZE

The selection of the BGE was based on the stability of the graphene oxide sheets in aqueous solution. The stability is affected by the ionic strength and pH of the BGE. The effect of different concentrations of ammonium acetate solutions, 2, 5 and 10 mM at a fixed pH of 7 were studied for the CZE analysis of the GOx (see Fig. 2). In less concentrated 2 mM electrolyte a single broad peak was observed in the electropherogram, whereas in 10 mM electrolyte a large number of very sharp peaks (spikes) were obtained. Using 5 mM electrolyte the electropherogram contained attributes of those observed using the more extreme concentrations.

In 2 mM ammonium acetate solution, aggregation of GO sheets is less likely to occur and the individual sheets migrate inside the capillary like ordinary molecules in CZE, based on their electrophoretic mobility. The charge and size distribution of the non-aggregated nanosheets causes the overlap of their migration times resulting in a broad peak. The appearance of spikes is due to the aggregation of GO sheets with increase of electrolyte concentration as we reported earlier [15]. CZE of suspensions of another carbon nanostructure, carbon nanotubes, resulted in electropherograms with a similar occurrence of spikes which are assumed to be caused by aggregates of carbon nanotubes [6,7]. In general, spikes occur when the ionic strength of the BGE was increased. The spikes in the electropherograms were irreproducible as aggregation occurs randomly. These results demonstrate remarkably well how the electrolyte concentration can lower the repulsion potential and increase the aggregation probability of two colliding sheets. The electropherograms in Fig. 2 clearly show that single nanosheets (2 mM) have a lower mobility than the bigger aggregates (10 mM).

For the CZE analysis of GO samples, it is critical to choose a low ionic strength BGE that will not induce aggregation. In order to run at a higher pH where we could better ionise the sheets, we replaced ammonium acetate with tetrapropylammonium hydroxide as supporting electrolyte. At a concentration of 250 μM, the pH of the resulting solution was 10.4. The CE current obtained was also comparable to that obtained with the 2 mM ammonium acetate. Ammonium hydroxide was not used because we observed instability of the graphene samples in this base.

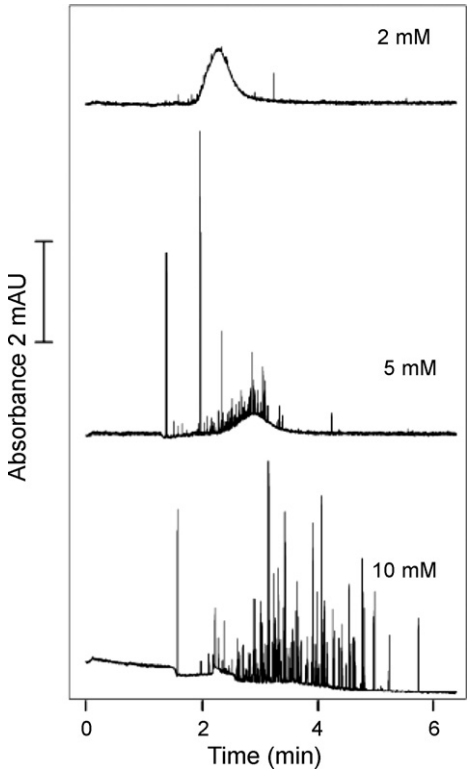

Fig. 2. CZE separation of GOx sample using different concentrations of ammonium acetate as background electrolyte (from top to bottom 2, 5 and 10 mM) at a fixed pH of 7. See Section 2 and text for details.

3.2. CZE of GO water dispersions

3.2.1. Exfoliation of graphite oxide

Fig. 3 shows the electropherograms from the CZE analysis of the GO labeled samples. In general, more spikes are observed with the larger sheets (i.e., GO0 and GO1), and the spikes almost disappeared as the size of the sheets become small (i.e., GO3 and GO3a). The spikes are reminiscent of the spikes observed from the sheet aggregates in the previous study using the higher concentration of ammonium acetate as BGE. All spikes in the electropherograms are considered to be aggregates that are stacks of graphene nanosheets and therefore big enough to cause a spike by the detector. This is also consistent with the spikes observed in the CE analysis of single 200–1000 nm sized sulphated polystyrene particles [23].

From the electropherograms, where GO3 or GO3a show very little aggregates, we conclude that exfoliation of oxidized graphite to smaller sheets is almost complete after sonication at 50% power for 15 h. It should be noted that centrifugation of sample GO3 produced a smaller broad peak (compare electropherogram for GO3 and G3a). This is caused by the decrease in the concentration of the sheets in GO3a due to extraction by centrifugation.

3.2.2. AFM analysis of CZE fractions of GO1

In order to verify the existence of individual sheets or aggregates in the peaks or spikes in the electropherograms in Fig. 3, we collected CZE fractions obtained from GO1 and subjected them to AFM analysis. Since each CZE run produces nanoliters of separated nanosheets in dispersion, the injection time was increased to 80 s at 50 mbar and fractions were collected from more than 60 sample injections. The CZE profile of the longer injection was quite different from the 5 s injection, thus four representative fractions were collected (see Supplementary Information Figure 2). The fractions

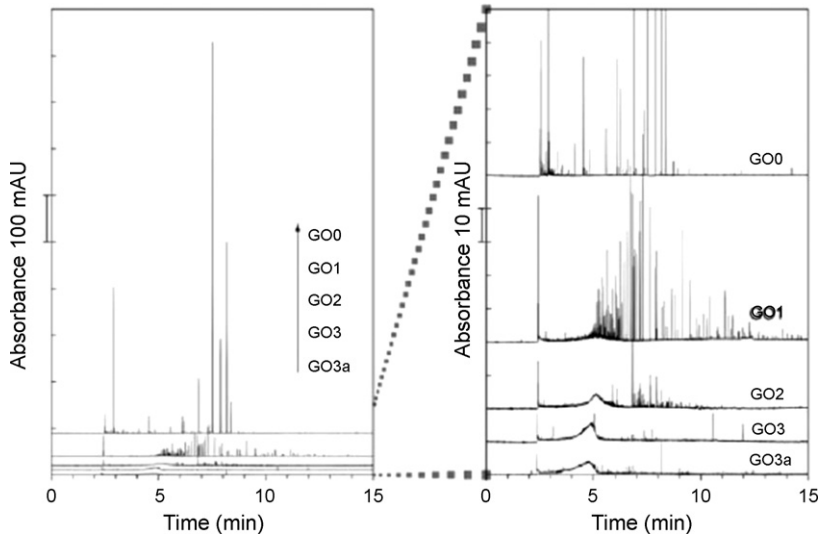

Fig. 3. CZE of GO samples (size of sheets from bottom to top: small to big). The right graph is a magnification of the left graph. See Section 2 and text for details.

were named A, B, C, and D that corresponds to the fractions collected between 0 and 2.5 min, 2.5 and 6 min, 6 and 7, and 7 to >10 min. Fraction A was from the start of the CE run to 0.5 min right after the detection of the EOF. This means that the eluted components at the EOF were collected in fraction A. Fraction B covered the main broad peak that corresponds to the exfoliated GO sheets, C the tail of the main broad peak and the sharp peak after the broad main peak observed from the longer injection of sample, and D the fraction that elutes after 7 min. Fractions C and D were believed to contain the non-exfoliated graphene oxide sheets that caused the spikes in the pertinent electropherogram shown in Fig. 3.

The resulting fractions were drop cast onto cleaned silicon wafer and air-dried. AFM images of the dry samples showed sheets for all fractions (see Supplementary Information Figure 2). It was interesting to see sheets coming out at the EOF time and this could be the uncharged sheets. It was not possible at this stage to distinguish the individual sheets from the aggregates due to difficulty in preparing the samples for AFM (i.e., reaggregation of graphene nanosheets tends to occur during drying of the deposited sample on silicon wafer).

3.2.3. Reduction of GO

Fig. 4 shows the electropherograms obtained for CCG0, CCG1, CCG2, CCG3, and CCG3a that was prepared from the reduction of GO0, GO1, GO2, GO3, and GO3a, respectively. The EOF time was around 2.5 min and the occurrence of a sharp peak at the EOF time suggests the presence of neutral graphene sheets. The broad peak at around 4 min for CCG2, CCG3, and CCG3a corresponds to the CCG sheets. These sheets were not observed for the samples that originated from GO solutions that were not sonicated at 50% power for at least 1.5 h. The amount of CCG sheets produced also depends on the time of sonication. Note that only a small peak was observed for CCG2 compared to CCG3 or CCG3a which was sonicated 10 times longer. A smaller broad peak was obtained for CCG3a compared to CCG3 due to the removal of some sheets in CCG3a that was obtained after centrifugation of CCG3. In addition, aggregation occurs randomly and we speculate that this caused the spike at the end of the broad signal for CCG3a. A similar but smaller spike could also be seen for CCG3.

3.2.4. Aggregation of CCG

In addition to monitoring the exfoliation of graphite to GO sheets and reduction of GO to CCG, we used the simple CZE method to follow the postreduction colloid quality of CCG over time. Fig. 5 shows electropherograms obtained from the reduction of CCG2

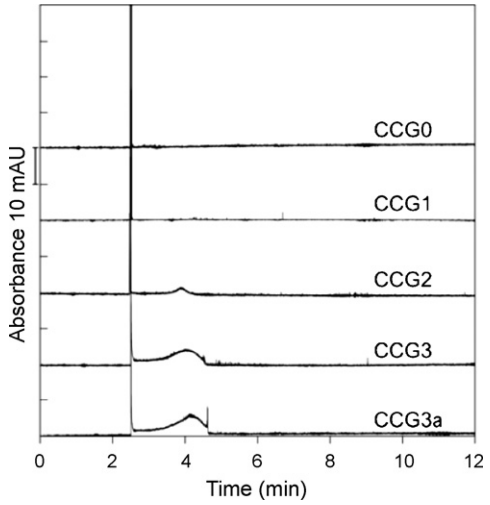

Fig. 4. CZE of CCG samples (size of sheets from top to bottom: big to small). The samples were obtained by hydrazine reduction of the GO samples from Fig. 3. See Section 2 and text for details.

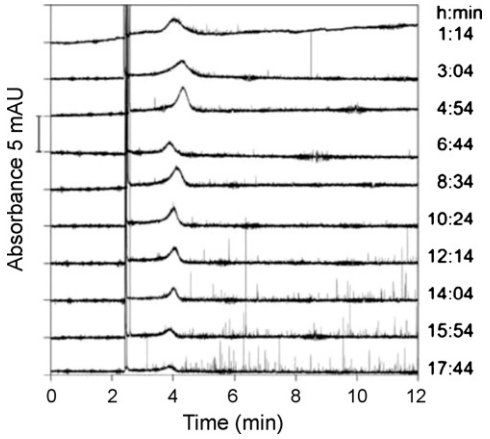

Fig. 5. Electropherograms of CCG2 at various times after hydrazine reduction. The numbers at the right of the figure represent the time when the sample was injected. See Section 2 and text for details.

with hydrazine after ~1 h to up to ~18 h. The amount of colloidal CCG decreases slightly after they have been reduced by hydrazine, and after 10 h we can observe the aggregates as spikes detected in the electropherograms. The reduction of CCG reduces the charges around the sheets which cause them to aggregate.

In the presence of an electric field, the injected nanosheets can be separated, while strong aggregation takes place due to orientation, even at low concentrations of BGE. In case of charged nanoplatelets the electrocoagulation occurs due to their forced coplanar orientation in electric field but not because of the reduction of the net surface charge. The nanosheets have non-charged neutral epoxy- and hydroxy-functional groups at the basal planes and charged carboxyl groups at the edges. Thus coplanar orientation should not reduce total electrostatic repulsion between negatively charged nanoplatelets, but promotes the van der Waals interactions between planes. This orientated electrocoagulation is different from common chemical or electrical coagulation where coagulation is caused by weakening electrostatic repulsion [16].

The possibility of aggregation due to the conductivity of the CCG sheets has been tested in a separate experiment but was not confirmed using the current experimental design. Two from the CCG dispersion isolated needles where inserted into an approximately 5 cm long thin glass tube (ID ~1 mm). The CCG dispersion did not visibly aggregate after 6 min of applying a voltage difference of 20 kV on the needles.

4. Conclusions

A CZE method that successfully monitored the exfoliation and reduction reactions involved in the preparation of CCG was described. Dispersion quality can be determined by CZE as proper exfoliation of GO results in a broad peak in the electropherogram whilst aggregates result in spikes. The CZE method will be employed as a valuable analytical technique during the preparation of CCG.

Acknowledgements

MBM thanks the Australian Research Council Nanotechnology Network (ARCNN) for financial support. JPQ and PNN acknowledge the Institutional Research Grants Scheme (IRGS) grant scheme of the University of Tasmania for the financial support of MBM visit and work in ACROSS. The authors thank the Australian Research Council for financial support.

Appendix A. Supplementary data

Supplementary data associated with this article can be found, in the online version, at doi:10.1016/j.chroma.2010.09.069.

References

[1] S. Stankovich, D.A. Dikin, R.D. Piner, K.A. Kohlhaas, A. Kleinhammes, Y. Jia, Y. Wu, S.T. Nguyen, R.S. Ruoff, Carbon 45 (2007) 1558.
[2] C. Quang, S.L. Petersen, G.R. Ducatte, N.E. Ballou, J. Chromatogr. A 732 (1996) 377.
[3] F.-K. Liu, J. Chromatogr. A 1216 (2009) 9034.
[4] N.G. Vanifatova, B.Y. Spivakov, J. Mattusch, R. Wennrich, Talanta 59 (2003) 345.
[5] Y.H. Rezenom, A.D. Wellman, L. Tilstra, C.D. Medley, S.D. Gilman, Analyst 132 (2007) 1215.
[6] S.K. Doorn, R.E. Fields, H. Hu, M.A. Hamon, R.C. Haddon, J.P. Selegue, V. Majidi, J. Am. Chem. Soc. 124 (2002) 3169.
[7] S.K. Doorn, M.S. Strano, M.J. O'Connell, E.H. Haroz, K.L. Rialon, R.H. Hauge, R.E. Smalley, J. Phys. Chem. B 107 (2003) 6063.
[8] B. Suarez, B.M. Simonet, S. Cardenas, M. Valcarcel, J. Chromatogr. A 1128 (2006) 282.
[9] X.Y. Xu, R. Ray, Y.L. Gu, H.J. Ploehn, L. Gearheart, K. Raker, W.A. Scrivens, J. Am. Chem. Soc. 126 (2004) 12736.
[10] J.S. Baker, L.A. Colon, J. Chromatogr. A 1216 (2009) 9048.
[11] U. Pyell, Electrophoresis 29 (2008) 576.
[12] P.H. Wiersema, A.L. Loeb, J.T.G. Overbeek, J. Colloid Interface Sci. 22 (1966) 78.
[13] A.V. Delgado, F. González-Caballero, R.J. Hunter, L.K. Koopal, J. Lyklema, J. Colloid Interface Sci. 309 (2007) 194.
[14] U. Pyell, Electrophoresis 31 (2010) 814.
[15] D. Li, M.B. Muller, S. Gilje, R.B. Kaner, G.G. Wallace, Nat. Nanotechnol. 3 (2008) 101.
[16] H.Y. He, J. Klinowski, M. Forster, A. Lerf, Chem. Phys. Lett. 287 (1998) 53.
[17] A. Lerf, H.Y. He, M. Forster, J. Klinowski, J. Phys. Chem. B 102 (1998) 4477.
[18] T. Szabo, O. Berkesi, P. Forgo, K. Josepovits, Y. Sanakis, D. Petridis, I. Dekany, Chem. Mater. 18 (2006) 2740.
[19] H. Chen, M.B. Muller, K.J. Gilmore, G.G. Wallace, D. Li, Adv. Mater. 20 (2008) 3557.
[20] W.S. Hummers, R.E. Offeman, J. Am. Chem. Soc. 80 (1958) 1339.
[21] N.I. Kovtyukhova, P.J. Ollivier, B.R. Martin, T.E. Mallouk, S.A. Chizhik, E.V. Buzaneva, A.D. Gorchinskiy, Chem. Mater. 11 (1999) 771.
[22] C. Gomez-Navarro, R.T. Weitz, A.M. Bittner, M. Scolari, A. Mews, M. Burghard, K. Kern, Nano Lett. 7 (2007) 3499.
[23] C.F. Duffy, A.A. McEathron, E.A. Arriaga, Electrophoresis 23 (2002) 2040.